

Receivers for the Microwave Radiometer on Juno[©]

F. Maiwald, D. Russell, D. Dawson, W. Hatch, S. Brown, J. Oswald, M. Janssen

Jet Propulsion Laboratory, California Institute of Tech., Pasadena, CA, 4800 Oak Grove Drive, 91109, USA

Abstract — Six receivers for the MicroWave Radiometer (MWR) are currently under development at JPL. These receivers cover a frequency range of 0.6 to 22 GHz in approximately octave steps, with 4 % bandwidth. For calibration and diagnosis three noise diodes and a Dicke switch are integrated into each receiver. Each receiver is connected to its own antenna which is mounted with its bore sights perpendicular to the spin axis of the spacecraft. As the spacecraft spins at 2 RPM, the antenna field of view scans Jupiter's atmosphere from limb to nadir to limb, measuring microwave emission down to 1000-bar.

Index Terms — Dicke Switch, Low Noise Amplifier, Magnetic Shield, Microwave, Noise Diode, Receiver.

I. Introduction

The Microwave Radiometer (MWR) [1] is being developed for the Juno spacecraft, a polar orbiter around Jupiter due to be launched in August, 2011. Juno is a NASA New Frontiers Mission with the goal to determine the origin and evolution of Jupiter. The three main experimental objectives are to: 1) determine Jupiter's internal mass distribution by measuring gravity with Doppler tracking; 2) determine the nature of its internal dynamo by measuring its magnetic fields with a magnetometer; and 3) determine the deep composition and dynamics of the sub-cloud atmosphere by measuring its thermal microwave emission.

With MWR, the thermal microwave emission will be measured to address two key questions: How was Jupiter formed; and how deep are the atmospheric circulations? The element oxygen, which appears in Jupiter as water, is the key to understanding how Jupiter formed. The main task of MWR is to determine the amount of water present in the interior of Jupiter to within one, three, or nine times its solar abundance. These possible values discriminate among plausible models for the condensation of Jupiter from the early solar nebula. As described by Janssen et al. [1] to accomplish this goal, MWR must measure the dependence of Jupiter's brightness temperature to a view angle at 6 octively spaced frequencies from 0.6 to 22 GHz. The ratio of the off nadir brightness relative to the nadir brightness must be measured with an accuracy of 0.1 % at 1-sigma. This task requires stable receivers but does not depend on absolute gain calibration of the receivers.

Secondary goals are: 1) to measure the thermal emission at multiple angles to determine Jupiter's atmospheric dynamics [2]; and 2) to map synchrotron emission from the toroidal radiation belt centered above Jupiter's equator. Study of the latter requires a dynamic range of more than 40 dB for the two receivers with the lowest frequencies, 0.6 and 1.25 GHz. The synchrotron radiation peaks at 0.6 GHz and decays

exponentially with increasing frequency, becoming negligible for the receivers at 5.2 GHz and above.

In this publication the receiver subsystem will be described along with its performance.

II. Receiver Subsystem

A. Description of the receiver subsystem and requirements

The receiver subsystem contains six separately packaged receivers which are bolted together as one unit (see Figure 1). The receivers, identified as R1 through R6, have center frequencies of 0.6, 1.25, 2.6, 5.2, 10, and 22 GHz respectively. All receivers have an H-frame chassis that allows separation of the DC electronics from the sensitive RF signal chain. This setup provides maximum rejection of external noise while minimizing mass, a critical parameter for planetary missions.

A performance model of the MWR instrument was developed which includes the antennas, the RF transmission

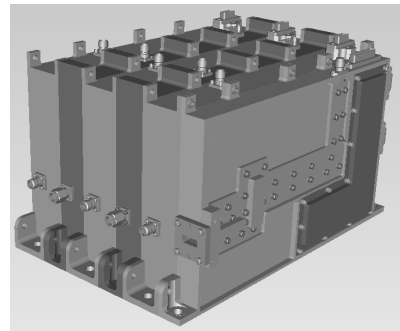


Fig. 1: Model of the receiver subsystem. On the left side the RF inputs are visible. A WR-42 waveguide is used at 22 GHz and all other receivers have coaxial connectors. The electric interfaces are on top and in the back located.

lines, and the receivers. With this model, a detailed analysis of all error contributions and their distribution was performed incorporating the measured capability of the prototype and Engineering Model (EM) receivers. As a result, a set of performance requirements for the receivers was defined. The key requirements are listed in Table 1.

In each receiver, up-screened commercial parts are employed. Custom-made parts are limited to isolators and bandpass filters. The MWR receivers have been developed in two phases. First, prototype models were used to determine which commercial components could meet the requirements. It was also determined which receivers would utilize either packaged (surface mount technology) or MMIC (hybrid) device and assembly approaches. Second, based on the

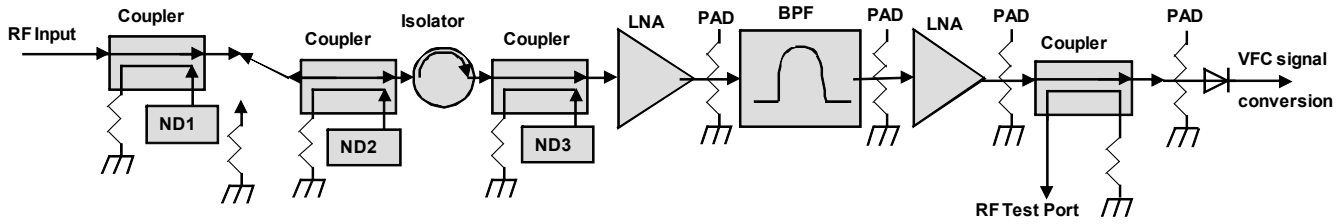


Fig. 2: Simplified receiver block diagram. Calibration is enabled by three integrated noise diodes and one Dicke switch. The isolator provides matching to the external components. The multiple filter stages form the bandpass and the LNA stages provide sufficient gain to detect the incident RF signal on the detector.

prototype development, the EM receivers were designed. In assembling the EM receivers, the designs, assembly processes, and key performance parameters were verified. The Flight Model (FM) designs and assembly processes were then modified and reviewed based on the EM results.

The receiver subsystem is located inside a shielded vault, which protects MWR from up to 12 kRad radiation during the first year of the science mission. Additionally, the vault provides thermal stabilization of MWR to within ± 2 K over the 2 hour perijove pass and a short term thermal stability of ± 0.1 K over 5 minutes.

B. Block diagram

The block diagram for a representative receiver is shown in Figure 2. The incident RF power for R1 through R5 is coupled from a 2.92 mm connector to a transmission line. R6 has a WR-42 waveguide port and a broadband E-plane waveguide probe which couple the incident power into a micro-strip line. These micro-strip lines as well as the other RF substrates are made of alumina for R4-R6. For R1-R3 the RF substrate material is TMM10I, a ceramic laminate from Rogers [3], with the exception of the couplers which are made of alumina. All RF substrates are bonded with epoxy to a gold plated aluminum. In order to verify the stability of the receiver, which is one of the key requirements (Req. 5) in table 1, its performance was measured repeatedly over a wide temperature range of -20°C to 50°C .

Three noise diodes and a Dicke switch are integrated in the front-end of each receiver for calibration and diagnostic purposes. The brightness temperature of each diode is attenuated to 150-350 K, referenced to the receiver input. Analyzing the receiver output for each noise diode allows comparison of different diode brightness temperature ratios over temperature and time. Using these ratios, the transmission can be tracked through the front-end to the first Low Noise Amplifier (LNA). Any changes which could result in calibration errors can be detected. The first noise diode is positioned next to the input connector followed by a Dicke switch. The Dicke switch is toggled between a 50 Ohm load, at the physical temperature of the receiver, and the antenna position. After the Dicke switch, a second noise diode is

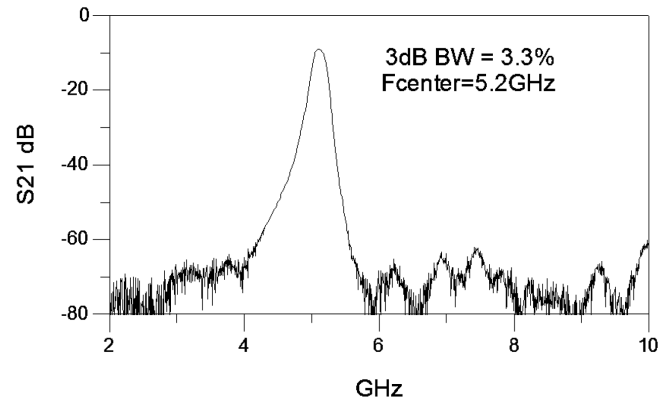


Fig. 3: Bandpass of the R4 receiver

integrated, followed by an isolator. Finally a third noise diode is placed between the isolator and the first LNA. Attenuator values between 2 dB and 8 dB are placed at the input and output of the amplifiers following the first LNA. This minimizes mismatch effects between the amplifiers and the bandpass filters. Several filter stages form a 4% wide bandpass at the receiver center frequency (Req. 1). The amplified signal is detected by a tunnel diode.

To achieve the required narrow bandpass (Req. 1), two thermally stable filter technologies are utilized. R1 to R3 employ evanescent mode filters (inductively coupled high Q) designed by RS Microwave [4]. The measured losses are about 3.8 dB within the bandpass and the filters have superb out-of-band rejection, better than -50 dB across the LNA bandwidth from 0 to 10 GHz. The rejection outside the bandpass is required to suppress the spillover of synchrotron radiation. R4-R6 use ceramic based micro-strip filters developed by DLI [5]. This material has a high dielectric constant, minimizing the receiver size. Multiple filters with successively narrower bandwidths are cascaded to define the required 4% bandwidth and -50 dB out-of-band rejection. In figure 3, the transmission of the R4 receiver is displayed. Each filter requires a cavity which is machined in the receiver's chassis. This cavity is sized to reduce sensitivity to the cover height as well as to suppress higher order modes from propagating through the filter cavity.

The number of required LNAs is defined by the attenuation

TABLE 1: Description of main performance requirements for the MWR receivers

Req.	Key Requirements	Comments
1	Receiver Bandpass	4 % bandwidth, out-of-band rejection better than -50 dB @ 10 % from carrier
2	Performance of noise diodes	Equivalent brightness temp dependence < 0.006 dB/C and < 0.05 % ENR repeatability
3	Receiver noise temperature	Receiver noise temperature
4	Input Return loss	Input impedance matching (VSWR), impacts radiometric offset and gain errors
5	Receiver Gain Stability	Stability of receiver gain 0.0001 integrated over 128 sec (Allan variance)
6	Receiver Dynamic Range	R1-R2 require 50 dB and R3-R6 require 30 dB dynamic range at the detector
7	Dicke Switch Isolation	Suppressing noise contribution due to synchrotron radiation in load position, > 25 dB
8	Magnetic susceptibility	Contribution on radiometric offset and gain errors due to external magnetic field

through the filters and RF attenuators as well as the required dynamic range (Req. 6). The amplified RF signal needs to be approximately -30 dBm, incident to the detector, in order to ensure a linear response with minimal impact from its own noise. To minimize thermally induced gain changes of the LNAs, each MMIC bias circuit is temperature compensated. The amplified RF signal is detected with a tunnel diode, delivering an output voltage of less than 10 mV. The detector output is then amplified, converted to a digital output by a voltage to frequency converter, and then transmitted to the Electronic Unit (EU) [6]. The EU counts the pulses over a 100 msec integration window to determine the average power. This value is then passed to the spacecraft computer.

C. Challenge

The magnetic field of Jupiter along the MWR orbit can be as high as 15 Gauss. The 2 RPM spin rate of the spacecraft is slow enough that Faraday induction can be neglected. However, the slowly varying, strong magnetic field modulates the RF performance of the isolator, a magnetic-susceptible component.

During the prototype development phase of the receivers the RF isolators were identified to be the only magnetic susceptible parts. The return loss, insertion loss, and isolation of the isolators were modulated with an applied magnetic field. As a result, the matching changed between the isolator and the first LNA. Additionally, the leakage of the correlated noise from the LNA in the direction of the antenna was modulated which was reflected back toward the receiver from the antenna interface. Both effects resulted in a significant error which was too complicated to be compensated for by calibration. A magnetic shield had to be developed to suppress the modulation. Magnetic shielding of each receiver or the entire receiver subsystem would compromise the performance of the spacecraft's magnetometer. Therefore, approaches to minimize the mass and package volume for the shielding were pursued. The shield was simulated with the magnetic module of Ansoft's HFSS and Maxwell to ensure: 1) minimum package volume, 2) minimum magnetic material usage, 3) minimal impact on isolator RF performance, and 4) no saturation effects. The outcome of these simulations was a compact

magnetic shield around the isolator. For the shield to match the modeled performance, good physical contact between shield components is required. For the three low frequency receivers (R1-R3) an interlacing "clamshell" was designed and for the three higher frequency receivers (R4-R6) a "shoe box" approach was used.

Each magnetic shield has two parts which enclose the isolator from the top and from the bottom. These shields provide sufficient metal contacts to ensure that 1) the magnetic fields of the isolators are enclosed within their shields, as well as 2) external magnetic fields are deflected. Additionally, the thickness of the shields needs to be at least 1 mm to avoid any magnetic saturation due to Jupiter's magnetic field and the field of the isolators.

III. Measurements and Results

In order to verify the RF performance against the requirements, the hardware was tested for the following: thermal stability, RF input matching, bandpass characteristics, magnetic susceptibility, and mechanical and electrical interface compatibility.

Most of the receiver's performance was characterized with radiometric measurements at selected temperatures from -20°C to +50°C. At these temperatures, the receivers were thermally stabilized and a calibration sequence incorporating various on/off states for the noise diodes and the Dicke switch was defined. Each configuration had a 100 msec integration time. The obtained radiometric data was recorded and analyzed. A subset of the main parameters: receiver gain stability (Req. 5), temperature dependence of the noise diode brightness (Req. 3), and dynamic range (Req. 6) are provided in table 2. During the EM phase the dynamic range of R4 and R5 receivers were verified with a newly developed calibration unit based on work performed by Peng et al. [7]. This unit provides a synthetically generated noise signal which is programmable in shape, bandwidth, and signal strength. It streamlines test efforts by determining the linearity over the entire dynamic range as well as calibrating the internal noise diodes in one compact test setup. For the FM phase, one calibration unit will be available for each receiver. A calibration target at 77 Kelvin and room temperature was used to calibrate the

TABLE 2

SUMMARY OF REQUIREMENTS AND MEASURED VALUES,

* R6 was not verified but the selected components are predicted to meet the requirements

Receiver	Req. 1	Req. 2	Req. 3	Req. 4	Req. 5	Req. 6	Req. 7	Mass & Power
#	%	dB/°C	K	dB	dG/G @ 30sec	[K]	dB	6.4kg, 19W
R1 (0.6GHz)	3.6	0.002	200	19	9.1E-5	0-18000	40	1.3kg, 3W
R2 (1.25GHz)	4.5	0.002	390	13	3.6E-5	0-5900	28	1.3kg, 3W
R3 (2.6GHz)	3.8	0.008	430	16	1.4E-4	0-1900	28.7	1.2kg, 3W
R4 (5.2GHz)	3.1	0.002	520	19	3.6E-5	0-700	40	0.9kg, 2W
R5 (10GHz)	3.8	0.003	600	17	1.5E-4	0-700	35	0.9kg, 4W
R6 (22GHz)*	3.0-4.0	<0.006	<972	>15	<1E-4	0-700	>25	0.8kg, 4W

internal noise diodes over temperature. The repeatability of the internal calibration sources was assessed repeatedly over temperature by monitoring the noise diode ratios (measured radiance from one diode relative to another) over temperature. The use of the noise diode ratios allowed potential variations in the external calibration source to be separated from anomalies internal to the receiver hardware itself. Anomalies induced by the thermal cycles could be detected from only a few hours of data. The inherent gain stability of the receivers was analyzed with an Allan variance plot. The EM measurements showed that the gain stability was better than required.

The remaining requirements on the RF input matching (Req. 4), the bandpass characteristics (Req. 1), the magnetic susceptibility (Req. 8) as well as the mechanical and electrical interfaces of the receiver were verified with different test setups. In the initial test phase, the interfaces were checked before RF performance characterization was performed. The input match was measured with a Vector Network Analyzer (VNA). The bandpass characteristic, requiring a 50 dB dynamic range, was verified with either a VNA or broadband noise source with a known output power. The magnetic susceptibility was measured on each receiver in the three main axes at room temperature using a Helmholtz coil. It was confirmed that with the implemented magnetic shields, the receivers were compliant with the requirements (Req. 8).

All receivers met the required performance with the exception of R6 which was not completely evaluated because of time constraints during the EM phase. However, based on measurements of individual R6 components it is expected that the requirements will be met.

IV. Conclusion

Extremely stable, space-qualified, microwave receivers for the MWR receiver subsystem have been developed. Power constraints, limited by the solar powered Juno spacecraft, was one of the key factors for selecting commercial RF components and the implementation approach of the RF and DC circuitry. The noise diodes in the front-end of the receivers provide an important tool for the calibration and diagnosis of receiver performance during implementation. With the

compact magnetic shields, the magnetic susceptibility of the isolators was reduced to negligible levels. A next step for future radiometric projects would be to miniaturize the receiver packages.

ACKNOWLEDGEMENT

The authors wish to acknowledge the assistance from Dr. H. Javadi, W. Chun, G. Bedrosian, and O. Montes on all RF measurements. Receiver assembly tasks were performed by M. Soria, A. Campbell, and C. Helizon-Flores. The machining was performed by H. Janzen and P. Bruneau. All mechanical designs and drafting were managed by D. Crumb.

The authors had very fruitful discussions and support from Dr. R. Menzies, Dr. T. Gaier, Annette Larson, and Dr. P. Stek on optimizing and managing the MWR receiver subsystem task.

The research described in this paper was carried out by the Jet Propulsion Laboratory, California Institute of Technology, under a contract with the National Aeronautics and Space Administration.

REFERENCES

- [1] M. A. Janssen, et.al. "Microwave Remote Sensing of Jupiter's Atmosphere from an Orbiting Spacecraft," *Icarus*, 173, pp. 447-453, 2005.
- [2] M. A. Janssen, *Atmospheric Remote Sensing by Microwave Radiometry*, New York: J. Wiley & Sons, 1993.
- [3] Rogers Corporation, Corporate Headquarters, One Technology Drive, Rogers, CT 06263
- [4] R.V. Snyder, "New Application of Evanescent Mode Waveguide for Filter Design", *IEEE Transactions: On Microwave Theory and Techniques*, December, 1977
- [5] DLI, Dielectric Laboratories Inc. 2777 Route 20 East, Cazenovia, New York, USA
- [6] P. Pingree, et.al., "Microwave Radiometers from 0.6 to GHz for Juno, A Polar Orbiter around Jupiter," *Aerospace Conf., IEEE Volume*, Issue , 1-8 March 2008 Page(s):1 – 15.
- [7] Peng, J., C. S. Ruf, "Calibration Method for Fully Polarimetric Microwave Radiometers Using the Correlated Noise Calibration Standard," *IEEE Trans. Geosci. Remote Sens.*, 46(10), 3087-3097, 2008.

© 2008 California Institute of Technology